Tetrahedron 74 (2018) 2202–2210

Contents lists available at ScienceDirect

Tetrahedron

journal homepage: www.elsevier.com/locate/tet

Enhanced enantioselective oxidation of olefins catalyzed by Mn-porphyrin immobilized on graphene oxide

Kayhaneh Berijani [a], Afsaneh Farokhi [a], Hassan Hosseini-Monfared [a, *], Christoph Janiak [b]

[a] Department of Chemistry, University of Zanjan, 45195-313 Zanjan, Iran
[b] Institut für Anorganische Chemie und Strukturchemie, Heinrich Heine Universität Düsseldorf, 40204 Düsseldorf, Germany

ARTICLE INFO

Article history:
Received 22 November 2017
Received in revised form
9 March 2018
Accepted 10 March 2018
Available online 13 March 2018

Keywords:
Asymmetric epoxidation
Graphene oxide nanosheets
Manganese-porphyrin
Enantioselectivity
Oxygen
Heterogeneous catalyst

ABSTRACT

An efficient enantioselective heterogeneous catalyst, GO-[Mn(TPyP)tart], was prepared by covalent attachment of Mn(III) complex of H_2TPyP via the propyl linkage to graphene oxide (GO) nanosheet and using chiral tartrate counter ion. The catalyst was characterized by Fourier transform infrared (FT-IR), diffuse reflectance ultraviolet–visible (DR UV–Vis) spectroscopy, powder X-ray diffraction (XRD), scanning electron microscopy (SEM), Raman and thermogravimetric analysis (TGA). The graphene-supported Mn-porphyrin showed higher activity for the enantioselective epoxidation of unfunctionalized olefins with molecular oxygen in the presence of isobutyraldehyde. It could be recovered easily and reused in asymmetric oxidation of styrene precursor in a five-step sequence without any considerable loss of its catalytic activity and selectivity. The obtained optically epoxide selectivities were achieved in 86% to 100%.

1. Introduction

Catalytic oxidation represents the basis of a variety of useful chemical processes for producing bulk and fine chemicals. One such process is the oxidation of olefins. Olefins oxidation reactions can be used for the production of essential precursors in organic synthesis such as alcohols, epoxides, aldehydes. Among these compounds, epoxides particularly chiral epoxides are useful and valuable intermediates with three membered ether ring structure that can undergo regioselective ring-opening reactions or transformation of functional groups. Chiral epoxides are used in chemicals industry, pharmaceuticals and agrochemicals.[1]

Asymmetric epoxidation is an important theme to convert olefins to chiral epoxides with high purity. These reactions can be commonly mediated with homogeneous transition metal complexes. However, wide spread applications of homogeneous catalysts are limited because of their high cost, difficulty in separation from the reaction mixture.[2] These drawbacks can be overcome by heterogenization of a homogeneous catalyst on solid supports. Furthermore, the stability, product selectivity and recovery of the catalyst can be improved in heterogenized form.[3] Consequently, there are a lot of efforts for design and synthesis of efficient heterogeneous catalysts especially for asymmetric oxidations.[4,5] Ti-chiral tartrates grafted on MCM-41 catalyze the epoxidation of styrene by *tert*-butyl hydroperoxide with reasonable enantioselectivity (55–62% ee).[6] Amine-catalyzed epoxidation of α, β-unsaturated aldehydes is enhanced by attaching the nanosheets of layered double hydroxides (LDHs) and the epoxide yield of 76% (93% ee) was obtained in the asymmetric epoxidation of cinnamaldehyde.[7] A new family of carbohydrate-based dihydroisoquinolinium salts has been as catalysts for the asymmetric epoxidation of olefins (57% ee).[8] New chiral Jacobsen's complexes attached to alkoxyl-modified ZPS-PVPA are active catalysts in the asymmetric epoxidations of unfunctionalized olefins with N-methylmorpholine N-oxide (high enantioselectivity and conversion).[9] The Mn complex of a N_4-tetradentate tetraamide macrocyclic ligand tethered onto Fe_3O_4@SiO_2 efficiently catalyzes the epoxidation of olefins by O_2/RCHO with selectivities 87–100% and 53–100% ee.[10] Heterogeneous catalysis is a key process in the manufacturing of a wide range of chemicals. It is at the heart of green chemistry and sustainable chemical processes. Among the used metal compounds, Mn-complexes are of the best catalysts which are active in the epoxidation of olefins as homogeneous or heterogeneous due to their low toxicity and high activity.[11,12] The catalysts of Mn are powerful species for the asymmetric oxidation

* Corresponding author.
E-mail address: monfared@znu.ac.ir (H. Hosseini-Monfared).

https://doi.org/10.1016/j.tet.2018.03.027
0040-4020/

of un-functionalized olefins.[13,14] Synthetic metalloporphyrins mimic natural cytochrome P-450 enzymes in catalytic properties.[15,16] However, the important problems of metalloporphyrins that act as cytochrome P-450 models are easy destruction during the reaction and difficult recovery from the reaction mixture.[17] To overcome the self-decomposition problem of metalloporphyrins during the oxidation reaction they are usually isolated from each other by immobilization on solid supports.

Among the various solid supports, monolayer nanosheets of graphene oxide (GO) are an excellent candidate that can be functionalized with different materials to support various homogeneous catalysts. GO is prepared from abundant and inexpensive graphite which shows the necessary feature of high surface area for a catalyst immobilization and site isolation. Two-dimensional structure of GO allows catalytic species to be dispersed and as a result the mass transfer facilitated in the reaction processes.[18,19] However, there are some reports showing a decrease in the activity of the immobilized homogeneous catalysts.[20] One fascinating point about GO is the possibility of formation of hole defects during the GO synthesis with CO_2 production which enhance catalytic activities and also affect the shape or chemo-selectivity.[21] The numerous of porphyrin/graphene oxide nanohybrids have been synthesized with covalent and noncovalent approaches[22] and used in epoxidation olefins with various oxidants in oxidative reactions. For environmental considerations, one major goal in the oxidation reactions is the replacement of classical toxic waste-producing oxidants such as MnO_2 and $K_2Cr_2O_7$ with environmentally benign oxidants. Molecular oxygen is an environmentally clean terminal oxidant with high oxygen content (50%) that is free, easy to handle reagent with respect to H_2O_2 and without byproducts.

Herein we report on hybrid catalyst GO-[Mn(TPyP)tart], where [Mn(TPyP)tart] is manganese-tetra(pyridylporphyrine)tartrate. It was prepared via the covalent grafting of a Mn-porphyrin complex onto graphene oxide and its catalytic performance investigated in the enantioselective epoxidation of various unfunctionalized olefins with O_2. The catalyst is recyclable and showed high activity and enantioselectivity due to the synergistic interactions between GO and Mn-porphyrin.

2. Results and discussion

2.1. Characterization of the heterogeneous catalyst

GO[23] and chloropropyl functionalized graphene oxide, GO-Cl,[24] were synthesized by following reported procedures. Catalyst GO-[Mn(TPyP)tart] was synthesized and characterized by FT-IR, XRD, SEM, Raman, DR UV–Vis, TGA and AAS. Graphene oxide shows great potential as a support with complexation-ability for various catalysts due to its high specific surface area and accessible ample oxygenated functional groups. The Mn-porphyrin was attached to GO-Cl by a covalent bond between the N atom of the pyridyl and C atom of the propyl chloride groups (Scheme 1). Then, the axial acetate ligand of the Mn-porphyrin and the chloride counter ion both were exchanged by chiral tartrate anion. The asymmetric tartrate anions create a chiral environment around the Mn and porphyrin pyridyl groups. The resulting GO-[Mn(TPyP)tart] was an efficient and recyclable catalyst for the aerobic enantioselective oxidation of olefins.

2.2. FT-IR analysis

The chemical changes during preparation of the catalyst were monitored by infrared spectroscopy. Fig. 1 shows the FT-IR spectra of the starting materials and catalyst. The FT-IR spectrum of GO (Fig. 1a) shows a broad peak with strong intensity at 3417 cm^{-1} due to the O-H bonds. It reveals the presence of abundance of hydroxyl groups in GO. A shoulder at 3611 cm^{-1} is related to the weak hydrogen bonded O-H groups of GO. The appearance of new bands in the region of 2851, 2920[26] and 2958[27] cm^{-1} can be assigned to the C-H asymmetric and symmetric stretching bonds. The bands at 1737 and 1622 cm^{-1} are due to the C=O group of carboxylic acid and stretching vibration of –C=C group, respectively.[28] The vibration of C-O of carboxyl groups appears at 1423 cm^{-1}.[29] The new vibrational signature at about 1284 cm^{-1} attributed to asymmetric C–O–C stretching of the ether and epoxide groups.[30,31] The band at 1229 cm^{-1} represents the C-OH groups.[32] The characteristic bands at 1000 and 1051 cm^{-1} confirm the presence of the epoxy groups (C-O-C) complying with the symmetric stretching, asymmetric stretching, respectively.[28,33,34] In GO-Cl, the bands of methylene and methyl C-H stretchings are seen at 2851, 2920, 2958 cm^{-1} with increased intensity with respect to GO. The appearance of two strong bands at 1033 and 1118 cm^{-1} are characteristic of the vibrational stretching of Si–O–C and Si–O–Si bonds, respectively.[35]

The FT-IR spectrum of GO-[Mn(TPyP)tart] showed the C=N vibration at 1462 cm^{-1} in Fig. 1. The bands about 1400 cm^{-1} (1410-1343) correspond to symmetric vibration of the C=O groups.[36] By immobilization of the porphyrin onto GO-Cl, a new peak appeared at~1586 cm^{-1} due to the C=C and C=N vibrations.[37] The C=C stretching was observed around 1630 cm^{-1}.[68] The peaks at 1586 and 1630 cm^{-1} are attributed to the pyridyl C=C groups.[38] In comparison with GO-[Mn(TPyP)OAc], an increase in the ratio of the intensity of the peaks at 1729 and 1410-1343 cm^{-1} to the peak at 1586 cm^{-1} indicates the replacement of Cl and acetate (OAc) anions by tartrate anion (tart).[67]

2.3. XRD analysis

The X-ray diffraction patterns (Fig. 2) were used to investigate of the changes in the structure of GO, GO-Cl and GO-[Mn(TPyP)tart]. In diffraction pattern of pristine graphite powder there is an intense peak (002) at $2\theta = 26.37°$ (not shown in Fig. 2) corresponding to the *d*-spacing of 0.33 nm (layer-to-layer distance).[39] With the oxidation of graphite to GO, the basal reflection (002) shifted to lower angle (2θ = around 10°) with *d*-spacing of around 0.80 nm. Decreasing in 2θ and increasing the *d*-spacing indicate the formation of oxygen-containing functional groups such as carboxylic acid and hydroxyl on basal plane of graphite moiety (Fig. 2a).[40] In GO-Cl, a wide peak with low intensity appeared at $2\theta = 15–26°$ which attributed to alkylated GO with amorphous silica (Fig. 2b). Finally, The XRD pattern of GO-[Mn(TPyP)tart] displayed reduced peak intensities in comparison with the two other samples Fig. 2c. The results suggest the preservation of GO nanostructure during the synthesis of catalyst[28] and decreasing the intensity of peaks confirm the immobilization.

2.4. UV–Vis analysis

The UV–Vis spectra of the synthesized GO and GO-Cl indicate that how many degrees remained from the conjugate system.[23] The spectrum of GO indicates a maximum absorbance at 239 nm which corresponds to $\pi \rightarrow \pi^*$ of the aromatic C=C bonds (Fig. S1 (a)) and a shoulder at about 300 nm which relates to $n \rightarrow \pi^*$ transitions in the C=O bonds. In GO-Cl, a new peak appeared at 282 nm due to functionalization of GO (Fig. S1(b)).

Considering the insolubility of the GO-anchored Mn-porphyrin in common organic solvents so solid diffuse reflectance UV–Vis spectrophotometry was used to study electronic transitions. A typical Soret band with high intensity at 466 nm and two weaker Q bands appeared at 572 and 616 nm. The red shift of the Soret band

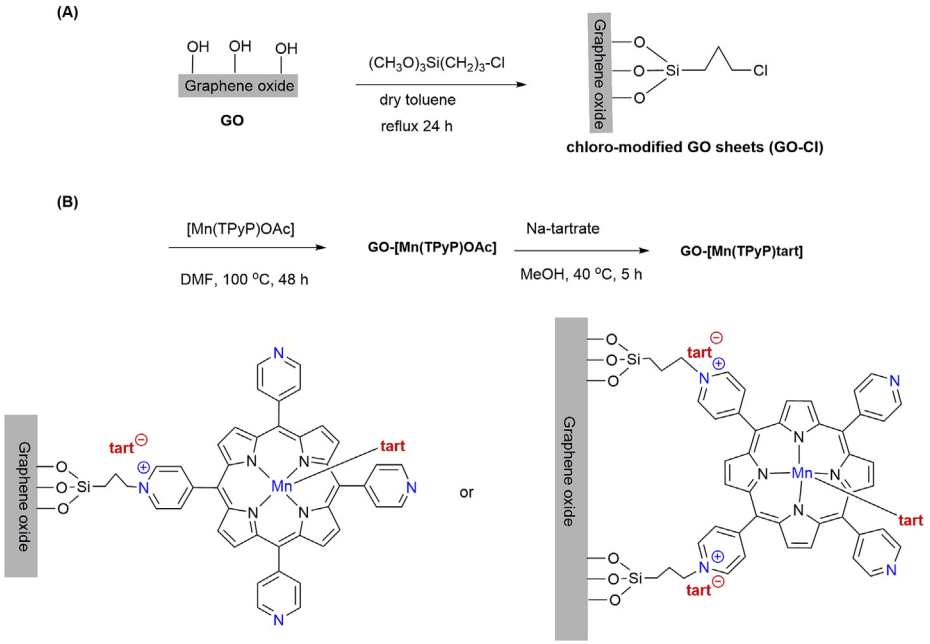

Scheme 1. The synthesis method for (A) GO-Cl and (B) chiral catalyst GO-[Mn(TPyP)tart]. The nanosheets of graphene oxide with random orientation[25] are represented by a rectangular box for simplicity.

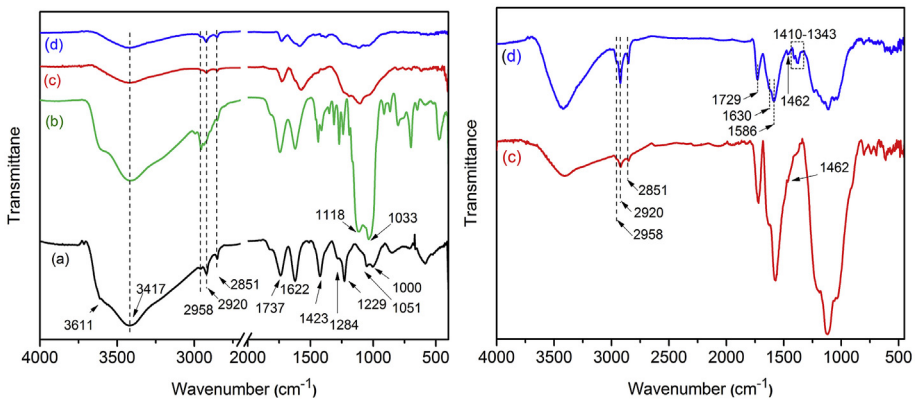

Fig. 1. The FT-IR spectra of (a) GO (b) GO-Cl (c) GO-[Mn(TPyP)OAc] and (d) GO-[Mn(TPyP)tart]. Expanded spectra of (c) and (d) are shown in the right figure.

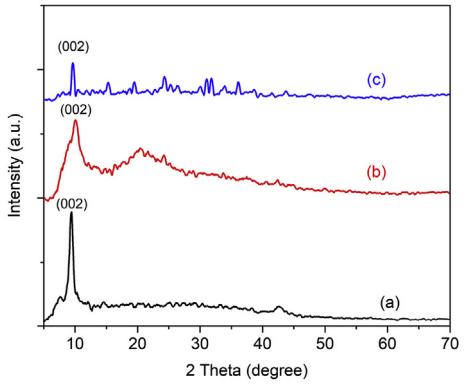

Fig. 2. XRD patterns of (a) GO (b) GO-Cl and (C) GO-[Mn(TPyP)tart].

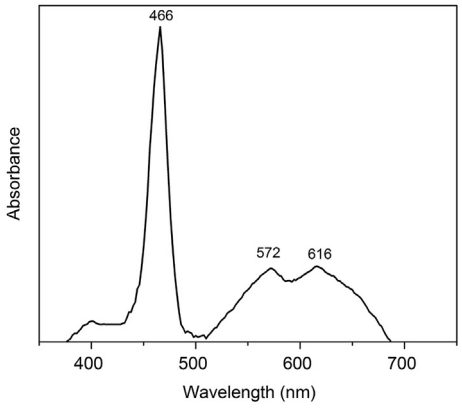

Fig. 3. DR UV–Vis spectrum of GO-[Mn(TPyP)tart].

with respect to its homogeneous counterpart (459 nm),[67] confirms the immobilization of [Mn(TPyP)OAc] onto the GO surface (Fig. 3).

This finding is a good document which indicates the changes in conjugation pathway and symmetry of a metalloporphyrin due to

the attachment on a support.[41–43]

2.5. Raman analysis

Raman spectroscopy is a useful and non-destructive characterization technique to investigate the ordered/disordered structure in graphene oxide nanosheets. In the Raman spectrum of pure graphite, a peak is seen at 1591 cm^{-1}, named G-band that is due to ordered sp^2-bonded carbon atoms but in GO, two well-known and typical vibration bands are observed.[44] In the Raman spectrum of the catalyst (Fig. 4), D-band appears at 1302 cm^{-1} that is generally assigned to the defects at sheet edges or disordered carbon due to the degradation of the sp^2 domains with the extensive oxidation.[45] The G-band peak at 1597 cm^{-1} corresponds to the high-frequency, Raman-active, E_{2g} mode of the vibrations of sp^2 carbons in graphitic hexagonal lattices.[39] The intensity ratio of D and G bands (I_D/I_G) is a criterion to assess the disorderness or defects in the sample species.[46] The ratio of I_D/I_G was 1.44 for GO-[Mn(TPyP)tart]; which is showing an increase of the defects concentration and a reduction in the crystallinity degree of GO.[47]

Comparison of the G band (1597 cm^{-1}) for GO-[Mn(TPyP)tart] with that of GO (1575 cm^{-1})[44] suggests an increase in the number of layers by immobilizing Mn-porphyrin on GO. One may conclude that the porphyrins are covalently attached on both sides of GO sheets and the linked porphyrins on two monolayer sheets can interact with weak π–π stacking interactions.[48]

2.6. SEM analysis

Fig. 5 shows the selected micrographs for graphite, GO and GO-[Mn(TPyP)tart]. In Fig. 5a the ordered flakes of graphite are seen. Wrinkling is seen clearly in nanosheets of GO (Fig. 5b). During the catalyst preparation, GO preserves wrinkled sheet texture nature without transformation (Fig. 5c). A little changes in the morphology of the catalyst with respect to that of GO can be related to the growing of steric hindrance by the covalent linkage of the porphyrin onto GO.[49]

2.7. Thermogravimetric analysis

The thermal behaviors of GO, GO-Cl and the catalyst were characterized by TGA. From the TGA and DTG curves, it can be seen that GO undergoes decomposition processes at several different temperatures. Based on the curve of GO (Fig. 6), the initial weight loss occurred at lower temperatures (below 100 °C) because the residual water was lost at the beginning. The second weight loss (38.55%) occurred at temperatures from 97 °C to 212 °C; it was attributed to the decomposition of the oxygen-containing groups of GO. The major weight loss from 212 °C to 621 °C was assigned to the breakdown of the -COOH group in GO.

For the GO-Cl curve, the weight loss below 104 °C was assigned to the loss of residual water and adsorbed solvent. The major weight loss (25.93%) occurred at the temperatures ranging from 104 °C to 278 °C, and it was attributed to the burning of the residual oxygen-functioned groups of GO-Cl. This weight loss is about 13% lower than that of the GO because of the functionalization by $(CH_3O)_3Si(CH_2)_3Cl$. The third weight loss at 277–560 °C was ascribed to the decomposition of the chloropropyl groups and carbon frame of the graphene. Therefore, the loading amount of 3-chloropropyltrimethoxysilane occupied about 16 wt% of the GO-Cl.

For GO-[Mn(TPyP)tart], the mild losing mass before 100 °C is evidently related to the adsorbed water. The significant degradation step at 225 to 308 °C is related to decomposition of labile oxygen functionalities.[50,51] The tartrate anions are probably decomposed in two steps at 308–420 °C and 420–595 °C. It should be notice that the porphyrin ring is stable up to 634 °C.[52] The major weight loss (19.57%) at the temperatures ranging from 225 to 308 °C is lower than those of GO (38.55%) and GO-Cl (25.93%). In addition, the maximum temperature of DTG peak is increased from 163 °C (GO) and 201.97 °C (GO-Cl) to 275 °C (GO-[Mn(TPyP)tart]). Both these findings confirm the immobilization of the Mn-porphyrin onto GO-Cl.

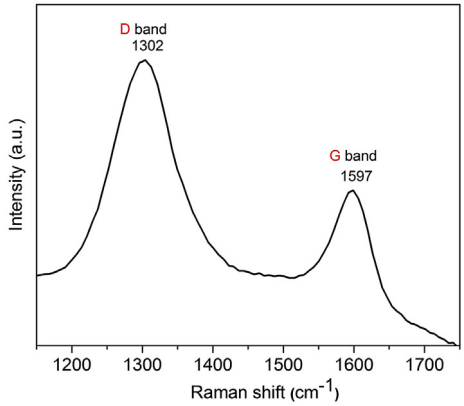

Fig. 4. Raman spectrum of GO-[Mn(TPyP)tart].

2.8. XPS analysis

The chemical composition of GO-[Mn(TPyP)tart] was characterized by XPS. The wide scan XPS spectrum of the catalyst is shown in Fig. S2 (in the supplementary). It displayed the sharp peaks at the binding energy of 285, 530, 101 and 199 eV, which were assigned to C 1s, O 1s, Si 2p and Cl 2p, respectively. The result indicated the existence of C, O, Si and Cl in the GO-[Mn(TPyP)tart] catalyst. The carbon 1s of GO including carbon sp^2, epoxy/hydroxyls, carbonyl, and carboxylates appeared at 285–289 eV.[53] The Na peaks are due to the presence of Na-tartrate or NaCl impurities. Also, in the XPS spectrum of Fig. S1, the N 1s for Mn-porphyrin located at 399.8 eV, representing for pyrrolic N.[54] All the results from the X-ray photoelectron spectroscopy (XPS) analysis demonstrated that the GO-[Mn(TPyP)tart] catalyst was prepared successfully. However, the Mn peaks are not seen in the XPS spectrum of the catalyst. Very weak peak for Mn-porphyrin has also been reported in the literature.[55] The analysis by atomic absorption spectroscopy also showed very low loading of the Mn-porphyrin on GO (20.28 μmol Mn/g catalyst).

2.9. Catalyst activity

The effectiveness of GO-[Mn(TPyP)tart] nanocomposite as a chiral catalyst was studied by the oxidation of olefins. Styrene was selected as model substrate for optimization of the reaction conditions. In this research O_2 and isobutyraldehyde were used as an oxygen source and a co-reactant, respectively.

The effect of the temperature was screened by the oxidation of styrene at 20, 40 and 60 °C (Table 1, entries 1–3). The temperature showed high effect on the yield, conversion and enantiomeric excess (ee). At 20 °C (Table 1, entry 1), the conversion, styrene oxide yield and ee values were low (17%, 12% and 33%, respectively). By increasing the temperature to 40 °C, the conversion of styrene was increased from 17% to 74%, however the reaction did not complete even after 8 h (Table 1, entry 2). The highest activity (conversion 100%) and selectivity (styrene oxide selectivity 89%, ee 73%) were achieved at 60 °C and the reaction completed after 2 h (Table 1,

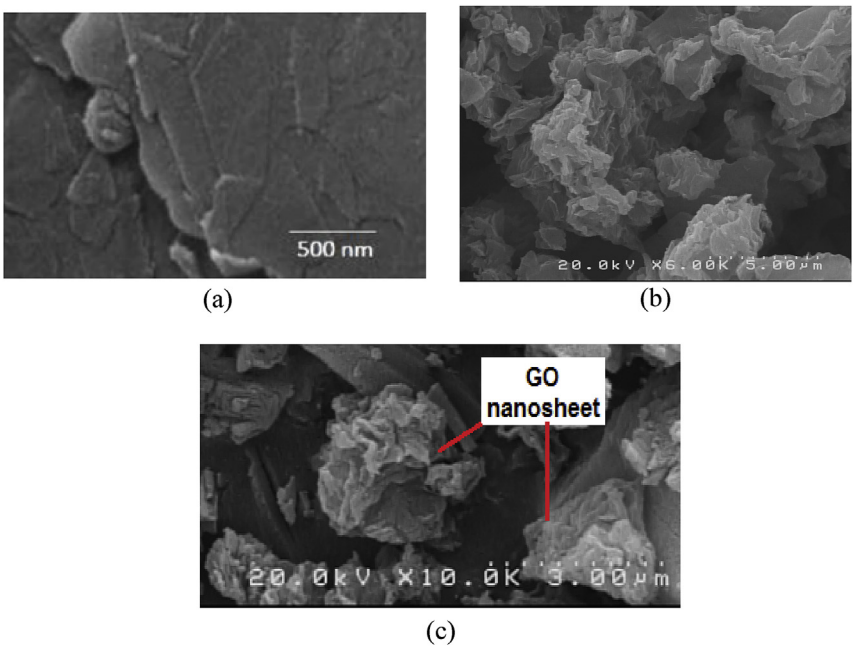

Fig. 5. SEM images of (a) graphite, (b) GO and (C) GO-[Mn(TPyP)tart].

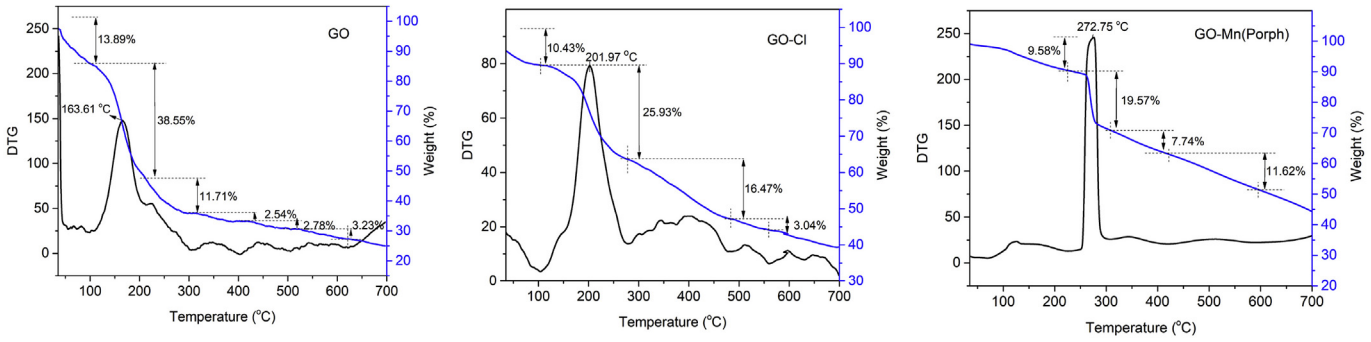

Fig. 6. Thermal gravimetric and DTG analysis of GO, GO-Cl and GO-[Mn(TPyP)tart].

Table 1
Effect of various parameters on the oxidation of styrene with O_2.[a]

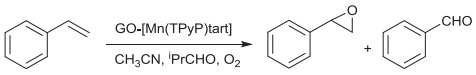

Entry	Catalyst	Solvent	Temp. (°C)	Time (h)	Conv.(%)[b]	Epoxide selectivity (%)	ee (%) (Conf.)[c]
1	GO-[Mn(TPyP)tart]	CH_3CN	20	8	17	71	33 (*S*)
2	GO-[Mn(TPyP)tart]	CH_3CN	40	8	74	70	54 (*S*)
3	GO-[Mn(TPyP)tart]	CH_3CN	60	2	100	89	73 (*S*)
4	GO-[Mn(TPyP)tart]	CH_3OH	60	2	0		
5	GO-[Mn(TPyP)tart]	EtOAc	60	2	48	54	31 (*S*)
6	GO-[Mn(TPyP)tart]	*n*-hexane	60	2	21	29	66 (*S*)
7	None	CH_3CN	60	2	0		
8	GO-[Mn(TPyP)tart] Without ^{i}PrCHO	CH_3CN	60	2	0		
9	GO	CH_3CN	60	2	0		
10	GO-Cl	CH_3CN	60	2	0		
11	GO-[Mn(TPyP)OAc]	CH_3CN	60	2	100	92	
12	[Mn(TPyP)OAc]	CH_3CN	60	2	100	88	

[a] Reaction conditions: catalyst 10.0 mg, styrene 2 mmol, ^{i}PrCHO 5 mmol, solvents (CH_3CN, CH_3OH, EtOAc and n-hexane) 5 mL, molecular oxygen 1 atm. The optimized conditions are denoted in underline.

[b] Conversions and yields are based on the starting substrate and determined by GC.

[c] Determined by GC on a chiral SGE-CYDEX-B capillary column. Absolute configuration of the epoxide of styrene was determined by comparison with the GC data with those observed for *R*-(+)-limonene.

entry 3).

Solvent nature was also studied for the enantioselective epoxidation of styrene in different solvents namely acetonitrile, methanol, ethyl acetate and *n*-hexane (Table 1, entries 3–6). It was found that acetonitrile is a favored solvent and gave excellent values of conversion (100%), styrene oxide selectivity (89%) and good ee% (73%) within 2 h (Table 1, entry 3). Using nonpolar *n*-hexane, polar protic (CH_3OH) or aprotic polar solvent (ethylacetate) resulted to lower activities and/or selectivity (Table 1, entries 4–6). These findings suggest that the polarity,[56] low coordinating ability and aprotic nature of acetonitrile play the main roles in improving the activity of catalyst GO-[Mn(TPyP)tart].

Control experiments proved that the oxidation of styrene by O_2/^{i}PrCHO is catalytic since in the absence of GO-[Mn(TPyP)tart] no reaction was ocurred (Table 1, entry 7). In the absence of isobutyraldehyde the reaction was not successful as well (Table 1, entry 8). Supporting agent GO and GO-Cl did not show catalytic activity (Table 1, entries 9 and 10). The oxidation of styrene in the presence of homogeneous [Mn(TpyP)OAc] and heterogeneous GO-[Mn(TPyP)OAc] catalysts, where the axial ligand is acetate anion and there is no tartrate anion as counter ion, resulted in complete conversion with high epoxide selectivities. However, there were no enantiomeric preferences between two enantiomers of the epoxide (Table 1, entries 11 and 12).

Catalyst GO-[Mn(TPyP)tart] showed noticeable potential for the epoxidation of aromatic, cyclic and linear terminal olefins with excellent epoxide selectivity (86–100%) and good enantioselectivity (58–100%) with O_2/RCHO (Table 2). The oxidation of aryl olefins were 100%. *Trans*-stilbene was oxidized to *trans*-stilbene oxide with retention of configuration and 58% ee. However, the oxidation of *cis*-stilbene gave *cis*-stilbene and *trans*-epoxide epoxide in the ratio of 20:80 (Table 2, entry 1). This finding suggests the involvement of a relatively stable radical intermediate that permits rotation around the C-C bond and conversion of *cis*-isomer to *trans*–isomer during the oxidation.[57] The completion of the epoxidation reaction at low time might be related to synergic effect between Mn(III)-Porphyrin and the GO support.[58]

In comparison to styrene, steric and electron withdrawing effects of the second phenyl on the olefinic C=C group increased the rate and epoxide selectivity (100%) in the oxidation of *cis*- and *trans*-stilbenes (Table 2, entries 1–3). The electron donor methyl group slightly decreases the epoxide selectivity (86%) and benzaldehyde yield in the oxidation of α-methyl styrene with respect to styrene (Table 2, entry 4). However, involvement of steric effect around the olefin double of bond α-methyl styrene cannot be excluded. TOF of 4930 was obtained for both styrene and α-methyl styrene. 1-Phenyl-1-cyclohexene was converted to the corresponding epoxide with 100% selectivity and 69% ee (Table 2, entry 5).

Interestingly, the catalyst could oxidize even the linear terminal olefins, 1-octene and 1-decene, which have the lowest activity. The conversions were reasonable with high epoxide selectivity and enantioselectivity (Table 2, entries 6 and 7). The moderate yield of 1-octene is not surprising since 1-octene is less prone to epoxidation.[59] Generally, terminal aliphatic olefins need longer reaction time for complete conversion.[60] The important point is that in the enantioselective epoxidation of the two used terminal olefins, the epoxide was obtained with an excellent selectivity (100%) and ee (>91%). For 1-octene TOF was 837 (entry 6). Their ee values can be attributed to proximity and easy access to chiral centers in the catalyst.

Epoxide selectivity and enantioselectivity of GO-[Mn(TPyP)tart]/^{i}PrCHO/O_2 in the oxidation of styrene is higher than Mn(chiral-salen)Cl/NaOCl/pyridine N-oxide,[61] GO-Mn(chiral-salen)Cl/NaOCl/pyridine N-oxide[61] and Mn-porphyrin with chiral [2.2] paracyclophane derivative/NaOCl.[62] In addition to the green nature of the present catalytic system (O_2), the enantioselectivity (86–100% ee), recyclability and simplicity of GO-[Mn(TPyP)tart] catalyst are favored over those of the reported catalysts.[6–10] The formation of *trans*-epoxide in addition to *cis*-epoxide in the oxidation of *cis*-stilbene (Table 2), suggests a radical chain mechanism for the formation of epoxide by GO-[Mn(TPyP)tart]/^{i}PrCHO/O_2. It is predicted that the oxidation of olefins by this system proceeds via the formation of an acylperoxy radical upon the reaction of isopropylaldehyde with the Mn^{III}-porphyrin; this results in the formation of an acylperoxo-Mn or high valent Mn=O intermediate very similar to Mn^{III}(salen)/isobutyraldehyde/O_2 system,[63,64] which oxidize olefin.

2.10. Catalyst reusability

For the development of advanced, cost-effective and mild industrial processes, catalyst stability in reusable experiments are crucial. To study the recyclability and stability of GO-[Mn(TPyP)tart], the oxidation of styrene was investigated in five reaction runs under the optimized conditions (Fig. 7). At the end of each reaction run, the catalyst was completely separated from reaction mixture by centrifugation, washed thoroughly with acetonitrile to get rid of the organic reactant molecules and dried at 60 °C. The catalyst was reused in repeated epoxidation reactions of fresh reactants. Through the examining the filtrate by AAS and UV–Vis, it was found that there is no manganese, manganese-porphyrin or free base porphyrin in each run (Fig. S3). Consecutive conversions of styrene were 100%. GO-[Mn(TPyP)tart] showed no loss of activity, decreasing of epoxide selectivity or ee even after five consecutive catalytic cycles. The results confirmed that GO-[Mn(TPyP)tart] is a stable and recyclable heterogeneous catalyst. The SEM and FT-IR did not show any significant difference in the structure of the used catalyst versus the fresh one (Figs. S4 and S5). A decrease in conversion was observed after six times recycle.

3. Conclusions

In summary, we have developed an efficient system with high activity (TOF up to 14792) for the aerobic enantioselective epoxidation of olefins by using chiral catalyst GO-[Mn(TPyP)tart] under mild reaction conditions. The catalyst was stable and could be easily recycled. Various aromatic and aliphatic epoxides were produced from the corresponding olefins with excellent selectivity, and high yields. Synergic effect of the GO and catalyst play critical role in enhancing the activity of [Mn(TPyP)tart].[58]

4. Experimental section

4.1. General

Graphite powder, (2R,3R)-(+)-tartaric acid (L-(+)-tartaric acid), 5,10,15,20-tetra(4-pyridyl)porphyrin (H_2TPyP) and the other reagents were purchased from Fluka and Aldrich companies and used as received.

Chromatographic experiments were performed on an HP Agilent 6890 gas chromatograph equipped with an HP-5 capillary column (phenyl methyl siloxane 30 m × 320 μm × 0.25 μm) with flame-ionization detector. The enantiomeric excess (ee%) was determined by a GC (HP 6890-GC) using a SGE-CYDEX-B capillary column (25 m × 0.22 mm ID × 0.25 μm). ^{1}H NMR spectra of the reaction mixture were collected on a Bruker 250 MHz spectrometer. The UV–Visible absorption spectra were recorded on a Shimadzu 160 spectrometer. DR-UV spectra were run on a Shimadzu–2550 spectrophotometer. The structure of the

Table 2
Enantioselective epoxidation of different olefins with O_2/RCHO and GO-[Mn(TPyP)tart].[a]

No.	Substrate	Conv.(%)[b]/time	Product(s)/(Yield%)[b]	Epoxide selectivity (%)	ee(%)[c] (Conf.)	TOF (h^{-1})[d]
1	*cis*-stilbene	100/10 min	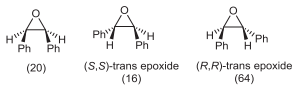 (20) (*S,S*)-trans epoxide (16) (*R,R*)-trans epoxide (64)	100	60 (*R,R*)	14792
2	*trans*-stilbene	100/10 min	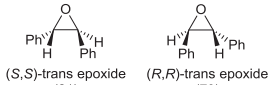 (*S,S*)-trans epoxide (21) (*R,R*)-trans epoxide (79)	100	58 (*R,R*)	14792
3	Styrene	100/2 h	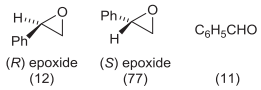 (*R*) epoxide (12) (*S*) epoxide (77) C_6H_5CHO (11)	89	73 (*S*)	4930
4	α-methyl styrene	100/2 h	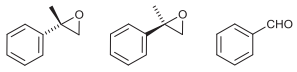 (*S*)-epoxide (76) (*R*)-epoxide (20) (4)	86	58 (*S*)	4930
5	1-Phenyl-1-cyclohexene	90/8 h	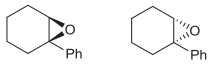 (*R,R*)-epoxide (14) (*S,S*)-epoxide (76)	100	69 (*S,S*)	1109
6	1-Octene	68/8 h	 (*R*)-epoxide (68)	100	100 (*R*)	837
7	1-Decene	23/8 h	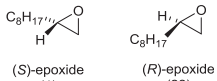 (*S*)-epoxide (1) (*R*)-epoxide (22)	100	91 (*R*)	283

[a] Reaction conditions: GO-[Mn(TPyP)tart] 10.0 mg (20.28 μmol Mn/g catalyst), substrates 2.0 mmol (except *cis*- and *trans*-stilbene 0.5 mmol), isobutyraldehyde 5 mmol, O_2 balloon 1 bar, CH_3CN 5 mL, 60 °C. Each experiment was repeated at least two times.
[b] All products conversion and yield were characterized through the GC analysis.
[c] The enantiomeric excess (ee) values were determined by the GC analysis on a chiral stationary phase (see the experimental section). The enantiomeric configuration of the major isomer was determined by comparing the GC data with those observed for *R*-(+)-limonene.
[d] TOF (turnover frequency) = (number of reacted molecules)/(active sites) (reaction time).

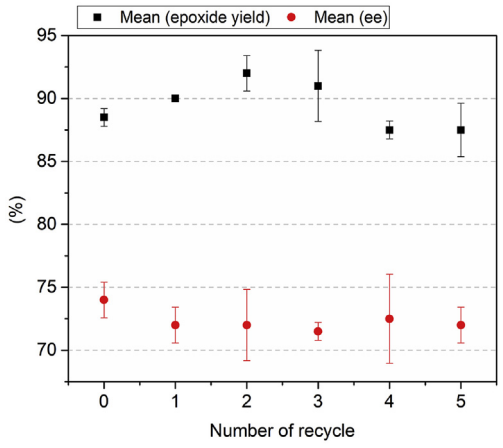

Fig. 7. The reusability of GO-[Mn(TPyP)tart] in the oxidation of styrene using O_2/^{i}PrCHO.

synthesized compounds was studied using Fourier transform infrared (FT-IR, Perkin-Elmer 597) spectrophotometer in the 4000-400 cm^{-1} frequency range using the prepared compounds diluted in KBr pellets. The X-ray powder profile (XRD) was recorded using Cu-Kα radiation, λα = 1.5406 Å, voltage: 40 kV, 40 mA, Bruker D8ADVANCE diffractometer, Germany. Scanning electron microscope (SEM, Hitachi F4160, voltage = 10 KV) was used to investigate morphology chemical composition of the prepared nanocomposite. Raman spectra were run on a RIGAKU spectrometer with laser power and wavelength 490 mW and 1064 nm, respectively. Thermogravimetric analysis (TGA) of the catalyst was investigated by Perkin Elmer Pyris Diamond. Manganese assay in the compounds were performed by a Varian spectrometer AAS-110.

X-ray photoelectron spectroscopy, XPS-(ESCA), measurements were performed with a Fisons/VG Scientific ESCALAB 200X spectrometer, operating at room temperature at a pressure of 1.0 × 10−8 bar and a sample angle of 30°.

4.2. Synthesis of [Mn(TPyP)OAc]

Complex [Mn(TPyP)OAc] was obtained from the metalation of H_2TPyP by Alder's method.[65] Briefly, 12.9 mmol of $Mn(OAc)_2 \cdot 4H_2O$ and 1.29 mmol H_2TPyP were dissolved in 100 mL of glacial acetic acid and heated at 80 °C for 6 h. After the completion of the reaction, the mixture was concentrated to dryness by a rotary evaporator. The residue was dissolved in 1000 mL of D.I. water at 60 °C. Then it was filtered and precipitated by the addition of sodium acetate solution (2 M). Yield: 81%.

UV–Vis (Fig. S6) in methanol: λ_{max} (ε, $dm^3\ mol^{-1}\ cm^{-1}$) = 459 (Soret, 85829), 559 (9598), 598 (2914). IR (KBr) spectrum (Fig. S7) showed the disappearing of ligand H_2TPyP bands at 3306 cm^{-1} due to N-H (pyrrole) and 1466 cm^{-1} due to C=N (pyridine and pyrrole).[66,67]

4.3. Synthesis of graphene oxide (GO)

GO was synthesized from graphite powder by using the modified Hummers method.[23] In a typical synthesis, a 10:1 mixture of concentrated H_2SO_4/H_3PO_4 (60:6 mL) was added to a mixture of graphite powder (0.5 g) and $KMnO_4$ (3 g). The reaction mixture was kept in an ice bath and stirred for 30 min and then heated at 70 °C for 24 h. Then, ice (60 g) and 35% H_2O_2 were added to the mixture. The resulting yellow suspension was washed consecutively with deionized water (30 mL), 30% HCl solution (30 mL), EtOH (200 mL) and diethylether (30 mL). The obtained GO was dried in the air.

4.4. Synthesis of GO-Cl

GO sheets were functionalized with propyl chloride following the reported procedure.[24] GO (0.33 g) was dispersed in dry toluene (23 ml) by sonication for 20 min. Then, the diluted 3-chloropropyltrimethoxysilane (1 mL in 6.5 mL dry toluene) was slowly added to the dispersion and heated under reflux for 24 h under nitrogen atmosphere. After cooling, the black powdery sample was filtered and washed for several times with toluene and EtOH to remove any impurities. The resulting GO functionalized by propyl chloride (shown as GO-Cl) was dried at 70 °C for 6 h.[68] Yield: 0.24 g.

4.5. Immobilization of [Mn(TPyP)OAc] on GO

The mixture of GO-Cl (0.1 g) and [Mn(TPyP)OAc] (0.01 g, 0.0137 mmol) in DMF (30 mL) was heated at 100 °C for 48 h under vigorous stirring.[69] After cooling the mixture to room temperature, the obtained black precipitate was washed with methanol (3 × 2 ml) and ether (2 ml). The resulting GO-[Mn(TPyP)OAc] was dried at 60 °C for 6 h. Yield: 96 mg.

4.6. Synthesis of Na-tartrate

For the synthesizing of the sodium tartrate salt, L-tartaric acid (0.1 g, 0.66 mmol) was stirred in 10 ml MeOH at 40 °C for 30 min. The pH of the solution was adjusted to 7 by dropwise addition of NaOH solution (1 M). The obtained white solid was filtered and thoroughly washed with MeOH (3 × 2 ml) and dried at 60 °C for 6 h. The identity of Na-tart was established by FT-IR. Yield: 90% (138 mg).

4.7. Synthesis of GO-[Mn(TPyP)tart]

A mixture of GO-[Mn(TPyP)OAc] (33 mg) and sodium-tartrate (50 mg, 0.206 mmol) in 15 mL methanol was stirred for 5 h at 40 °C. The resulting solid was exhaustively washed with methanol (3 × 2 ml) and DMF (3 × 2 ml) to remove the formed NaCl and NaOAc. At the end, the prepared GO-[Mn(TPyP)tart] was dried at 60 °C for 6 h.

The Mn-porphyrin loading on GO-[Mn(TPyP)tart] catalyst was determined by measuring the amount of Mn with atomic absorption spectrometry (20.28 μmol Mn/g catalyst).

4.8. Catalytic studies

The catalytic activity of GO-[Mn(TPyP)tart] was screened in the epoxidation of the selected unfunctionalized olefins with O_2 which was provided by an oxygen balloon (O_2,1 atm).

Typically, in a round bottom flask placed in an oil bath, the mixture of styrene (2 mmol), GO-[Mn(TPyP)tart] (10.0 mg) and isobutyraldehyde (5 mmol, 0.46 ml) as co-catalyst in acetonitrile (5 mL) was stirred for required time at determined temperature. After completion of the reaction, the catalyst was separated by centrifugation. The substrate conversion and yields of the products were quantitatively determined by GC-FID using a calibration curve. Enantioselectivity was determined using a chiral capillary column SGE-CYDEX-B. The configuration of the chiral products was assigned by comparison of the retention times in chiral GC with that of *R*-(+)-limonene.

4.9. Reusability test

The recycling experiments were achieved by repetitive use of GO-[Mn(TPyP)tart] in the epoxidation of styrene. After completion of the reaction and collecting the catalyst from the reaction mixture by centrifugation, the catalyst was washed thoroughly with 2 × 2 ml CH_3CN to remove the excess of organic compounds and dried at 60 °C for 6 h. It was reused for five consecutive runs. The probable leaching of Mn, Mn-porphyrin or porphyrin ligand was screened by employing atomic absorption and UV–Vis spectrophotometry. No remarkable leaching of the catalyst was detected in the reaction mixture. The nature of the recovered catalyst was investigated by FE-SEM and FT-IR.

Acknowledgments

The authors are grateful for the financial support of this study by the University of Zanjan.

Appendix A. Supplementary data

Supplementary data related to this article can be found at https://doi.org/10.1016/j.tet.2018.03.027.

References

1. Labinger JA. *J Mol Catal A Chem*. 2004;220:27–35.
2. Zhang A, Li L, Li J, Zhang Y, Gao S. *Catal Commun*. 2011;12:1183–1187.
3. Meunier B. *Chem Rev*. 1992;92:1411–1456.
4. Schrader I, Neumann S, Šulce A, Schmidt F, Azov V, Kunz S. *ACS Catal*. 2017;7:3979–3987.
5. Rodríguez-García L, Hungerbühler K, Baiker A, Meemken F. *J Am Chem Soc*. 2015;137:12121–12130.
6. Fadhli M, Khedher I, Fraile JM. *J Mol Cat A Chem*. 2016;420:282–289.
7. Zhe HL, He AJ. *Mol Cat*. 2017;443:69–77.
8. Philip C, Page P, Chan Y, Liddle J, Elsegood MRJ. *Tetrahedron*. 2014;70:7283–7305.
9. Huang J, Luo Y, Cai J, Chen X. *J Organomet Chem*. 2016;819:20–26.
10. Hadian-Dehkordi L, Hosseini-Monfared H, Aleshkevych P. *Inorg Chim Acta*. 2017;462:142–151.
11. Chatel G, Goux-Henry C, Mirabaud A, et al. *J Catal*. 2012;291:127–132.
12. Wang X, Miao C, Wang S, Xia C, Sun W. *ChemCatChem*. 2013;5:2489–2494.
13. Ito YN, Katsuki T. *Tetrahedron Lett*. 1998;39:4325–4328.
14. Jacobsen EN, Wu HM. In: Jacobsen EN, Pfaltz A, Yamamoto H, eds. *Comprehensive Asymmetric Catalysis*. vol. 2. Berlin: Springer; 1999:649.
15. Ishihara S, Labuta J, Van Rossom W, et al. *Phys Chem Chem Phys*. 2014;16:9713–9746.
16. Heier P, Förster C, Schollmeyer D, Boscher N, Choquet P, Heinze K. *Dalton Trans*. 2013;42:906–917.
17. Meunier B, de Visser SP, Shaik S. *Chem Rev*. 2004;104:3947–3980.
18. Szabó T, Tombácz E, Illés E, Dékány I. *Carbon*. 2006;44:537–545.
19. Zhao Q, Bai C, Zhang W, et al. *Ind Eng Chem Res*. 2014;53:4232–4238.
20. Zheng W, Tan R, Zhao L, Chen Y, Xiong C, Yin D. *RSC Adv*. 2014;4:11732–11739.
21. Su C, Acik M, Takai K, et al. *Nat Commun*. 2012;3:1–9.
22. Xu Y, Zhao L, Bai H, Hong W, Li C, Shi G. *J Am Chem Soc*. 2009;131:13490–13497.
23. Marcano DC, Kosynkin DV, Berlin JM, et al. *ACS Nano*. 2010;8:4806–4814.
24. Mungse HP, Verma S, Kumar N, Sain B, Khatri OP. *J Mater Chem*. 2012;22:5427–5433.
25. Zahed B, Hosseini-Monfared H. *Appl Surf Sci*. 2015;328:536–547.
26. Shao G, Lu Y, Wu F, Yang C, Zeng F, Wu Q. *J Mater Sci*. 2012;47:4400–4409.
27. Zhang Y, Fei D, Xin G, Cho UR. *J Compos Mater*. 2015;0:1–13.
28. Bhanja P, Kanti Das S, Patra AK, Bhaumik A. *RSC Adv*. 2016;6:72055–72068.
29. Acik M, Lee G, Mattevi C, et al. *J Phys Chem C*. 2011;115:19761–19781.
30. Acik M, Lee G, Mattevi C, Chhowalla M, Cho K, Chabal YJ. *Nat Mater*. 2010;9:840–845.
31. Acik M, Mattevi C, Gong C, et al. *ACS Nano*. 2010;4:5861–5868.
32. Pan D, Wang S, Zhao B, et al. *Chem Mater*. 2009;21:3136–3142.

33. Oh J, Lee JH, Koo JC, et al. *J Mater Chem*. 2010;20:9200–9204.
34. Lee DW, De Los Santos V, Seo JW, et al. *J Phys Chem B*. 2010;114:5723–5728.
35. Gao Y, Zhang Y, Qiu C, Zhao J. *Appl Organomet Chem*. 2011;25:54–60.
36. González-Mendoza AL, Cabrera-Lara Ll. *J Mex Chem Soc*. 2015;59:119–129.
37. Khatri PK, Choudhary S, Singh R, Jain SL, Khatri OP. *Dalton Trans*. 2014;43:8054–8061.
38. Zhu Y, Yu L, Wang X, Zhou Y, Ye H. *Catal Commun*. 2013;40:98–102.
39. Liu F, Sun J, Zhu L, Meng X, Qi C, Xiao F-S. *J Mater Chem*. 2012;22:5495–5502.
40. Zhang S, Zhu L, Song H, et al. *J Mater Chem*. 2012;22:22150–22154.
41. Li Z, Xia CG, Zhang XM. *J Mol Catal A Chem*. 2002;185:47–56.
42. Giovannetti R. In: Uddin J, ed. *Macro to Nano Spectroscopy*. vol. 1. Rijeka, Croatia: InTech; 2012:448.
43. Gouterman M. *J Mol Spectrosc*. 1961;6:138–163.
44. Bala Murali Krishna M, Venkatramaiah N, Venkatesan R, Narayana Rao D. *J Mater Chem*. 2012;22:3059–3068.
45. Stankovich S, Dikin DA, Piner RD, et al. *Carbon*. 2007;45:1558–1565.
46. Fu C, Zhao G, Zhang H, Li S. *Int J Electrochem Sci*. 2013;8:6269–6280.
47. Sunil M, Udaya Bhat K, Rahman MR, Jayalakshmi M. *Am J Mater Sci*. 2015;5:12–18.
48. Liu Y, Zhou J, Zhang X, et al. *Carbon*. 2009;47:3113–3121.
49. Chen L, Guo X, Guo B, Cheng S, Wang F. *J Electroanal Chem*. 2016;760:105–112.
50. Su H, Li Z, Huo Q, Guan J, Kan Q. *RSC Adv*. 2014;4:9990–9996.
51. Salavati-Niasari M, Bazarganipour M. *Appl Surf Sci*. 2008;255:2963–2970.
52. Lee KY, Lee YS, Kim S, et al. *CrystEngComm*. 2013;15:9360–9363.
53. Stankovich S, Dikin DA, Piner RD, et al. *Carbon*. 2007;45:1558–1565.
54. Liu L, Su L, Lang J, Hu B, Xu S, Yan X. *J Mater Chem A*. 2017;5:5523–5531.
55. Huang G, Yuan RX, Peng Y, et al. *RSC Adv*. 2016;6:48571–48579.
56. Gutmann V. *Coord Chem Rev*. 1976;18:225–255.
57. Adam W, Roschmann KJ, Saha-Möller CR, Seebach D. *J Am Chem Soc*. 2002;124:5068–5073.
58. Berijani K, Hosseini-Monfared H. *Inorg Chim Acta*. 2018;471:113–120.
59. Betz D, Raith A, Cokoja M, Kühn FE. *ChemSusChem*. 2010;3:559–562.
60. Klawonn M, Bhor S, Mehltretter G, Döbler C, Fischer C, Beller M. *Adv Synth Catal*. 2003;345:389–392.
61. Zheng W, Rong T, Yin S, et al. *Catal Sci Technol*. 2015;5:2092–2102.
62. Banfi S, Manfredi A, Montanari F, Pozzi G, Quici S. *J Mol Catal A Chem*. 1996;113:77–86.
63. Bryliakov KP, Khavrutskii IV, Talsi EP, Kholdeeva OA. *React Kinet Catal Lett*. 2000;71:183–191.
64. Katsuki T. *J Mol Catal A Chem*. 1996;113:87–107.
65. Adler AD, Longo FR, Kampas F, Kim J. *J Inorg Nucl Chem*. 1970;32:2443–2445.
66. Harriman A, Porter G. *J Chem Soc Faraday Trans*. 1979;75:1532–1542.
67. Berijani K, Hosseini-Monfared H. *Mol Catal*. 2017;433:136–144.
68. Nasseri MA, Allahresani A, Raissi H. *RSC Adv*. 2014;4:26087–26093.
69. Saeedi MS, Tangestaninejad S, Moghadam M, Mirkhani V, Mohammadpoor-Baltork I, Khosropour AR. *Polyhedron*. 2013;49:158–166.